Biophysical characterization of cochleate nanoparticles

PhD theses

Dr. Tamás Bozó

Semmelweis University
Doctoral School of Basic and Translational Medicine

Supervisor:	Dr. Miklós S. Z. Kellermayer, DSc., professor
Official referees:	Dr. Lívia Budai, PhD assistant professor Dr. Sándor Kunsági-Máté, PhD associate professor
Final Examination Comittee:	Dr. László Tretter, DSc., professor (Chairman) Dr. Krisztina Ludányi, PhD., associate professor Dr. László Grama, PhD, assistant professor

Budapest
2018

1. Introduction

Cohleates are Ca^{2+}-stabilized, spirally curving phospholipid membrane rolls with a typical length of a few micrometers and typical diameter of a few hundred nanometers. The interlamellar repeat distance of their multilamellar membrane structure is 5.1 nm, which indicates close packing of adjacent bilayers with no considerable aqeous space between them. The key step of cochleate formation is the interaction between phospholipids (in most cases phosphatidylserine, PS) and divalent cations (usually Ca^{2+}). Ca^{2+} ions form a 1:2 stoichiometry complex with PS, however the molecular details of their interactions are still not fully understood. Cochleates can be prepared by various methods, the common feature of which is that a (liposomal) suspension of negatively charged phospholipids is mixed with Ca^{2+} ions.

Cochleates are prospective drug-delivery vehicles and were found applicable to encapsulate and administer various active agents (e.g., *amphotericin B*, antibiotics, antitubercolotics, *miltefosine*, coagulation factor VIII, *raloxifen*). Nevertheless, in spite of their promising characteristics as drug carriers, cochleates have not been used in a single registered product yet, and the number of cochleate patents and publications are relatively low. We hypothesize that the reason for this stems from well identifiable shortcomings and technological problems of the field, among which *(1)* not fully understood mechanism of cochleate formation, and *(2)* aggregation of cochleates and their byproducts are the most important. Therefore, better knowlegde of cochleate formation and elaboration of a method to disperse aggregated cochleates are urgently needed to advance the development of cochleate drug-delivery vehicles.

2. Aims

My doctoral studies aimed at obtaining a better understanding on cochleate nanoparticles and developing technologies contributing to their application as drug-delivery vehicles. My objectives are summarized below:

(1) **Obtaining better understanding on the formation of cochleates:** I aimed at unraveling how cochleate membrane rolls evolve from unilamellar liposomes. Therefore, I decided to produce cochleates by mixing dioleoyl phosphatidylserine (DOPS) liposomes and Ca^{2+} ions and follow their formation by atomic force microscopy (AFM).

(2) **Structural and mechanical characterization of cochleates:** Former differential scanning calirometry and infrared spectroscopy studies suggested that upon Ca^{2+} addition PS molecules form a rigid, crystalline phase. However it is unknown how this phase transition affects the mechanical properties of phospholipid bilayers and the cochleate particle itself. I decided to elucidate the mechanical properties of cochleate membrane rolls, and characterize the topography and internal structure of individual cochleate particles by using AFM imaging and force spectroscopy.

(3) **Dispersion of aggregated cochleates:** Spontaneous and extensive aggregation of cochleate particles during their generation is the primary obstacle of development, analysis and application of cochleate drug-delivery systems. Therefore I aimed to develop a method to disperse aggregated cochleates without damaging their unique membrane roll structure.

3. Methods

3.1. Preparation of lipid systems

Multilamellar vesicle (MLV) suspension of 12.4 mM DOPS concentration was prepared by thin-film hydration technique. MLV suspension was extruded through a polycarbonate membrane filter to produce small unilamellar vesicles (SUV, d≈100nm). Cochleates were prepared by the addition of aqueous $CaCl_2$ solution to SUV-s via rapid mixing (for structural and nanomechanical studies) or dialysis (for dispersion studies). Nominal Ca^{2+} and DOPS concentrations of the samples were 6.2 mM.

3.2. Dispersion of cochleates

10 μl of the aqueous solutions of the tested potential dispersing agents (sodium acetate trihydrate, sodium tartaratetartrate dihydrate, trisodium citrate dihydrate, disodium edetate) prepared in a buffer containing 100 mM TRIS (pH 7.4) were added to 10 μl cochleate sample and mixed intensively by drawing through a narrow pipette tip 50 times. Samples were examined within 10 minutes after being mixed with dispersing agents. Control experiments were carried out with buffer only.

3.3. Structural and mechanical studies

Morphology of cochleate samples was studied by phase contrast and atomic force microscopy. Mechanical properties of cochleates were assessed by *in situ* AFM force spectroscopy. AFM images and force spectra were analyzed using the built-in algorithms of the AFM driver software. Internal structure of cochleate particles were analyzed by small-angle X-ray scattering (SAXS).

3.4. Characterization of surface charge and molecular interactions

To study the dependence of surface potential of DOPS membranes on Ca^{2+} concentration, zeta potential experiments were done. Molecular interactions between Ca^{2+} or dispersing agents and phospholipids were studied by ATR-FTIR spectroscopy.

4. Results

4.1.1. Cochleate formation

Ca^{2+} ion addition resulted in a concentration-dependent decrease of the absolute surface charge of SUV-s. Upon addition of $CaCl_2$ solution to DOPS liposomes at 1 to 1 molar ratio precipitation occurred due to formation of several-micron large, irregularly shaped aggregates (Figure 1. A). AFM imaging revealed that the resultant aggregates consisted of vesicles of various size, but no elongated structures resembling cochleates were seen (Figure 1. B).

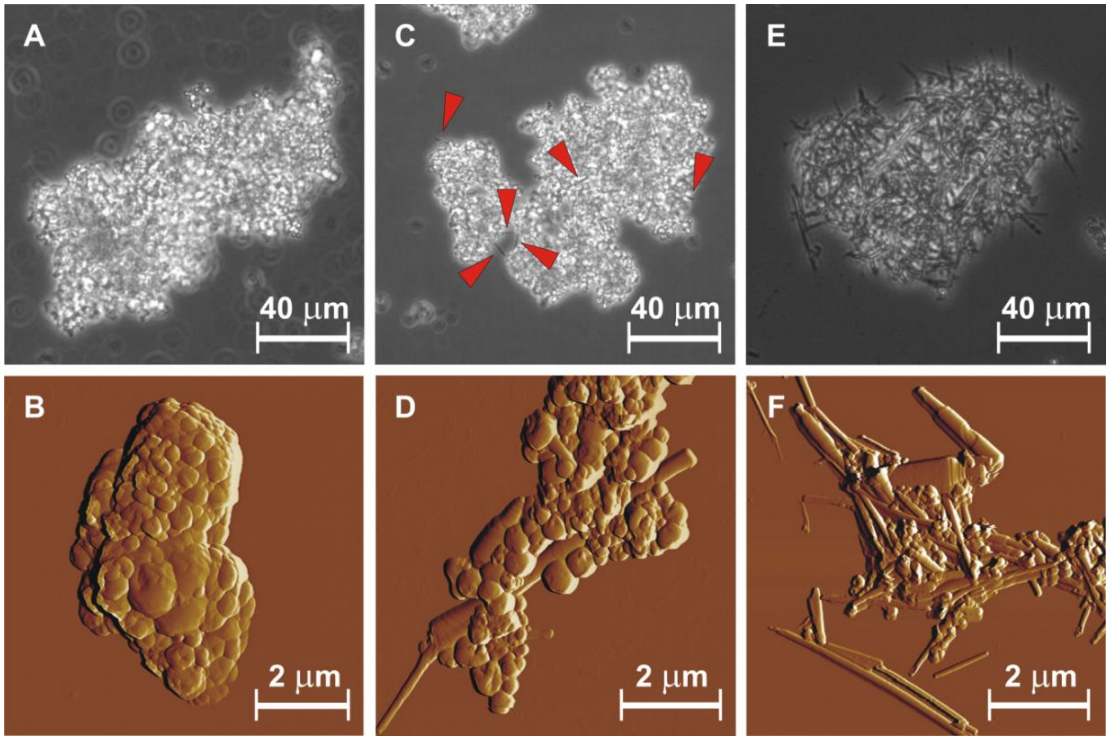

Figure 1. *Phase contrast microscopy (upper panels) and AFM amplitude-contrast images (bottom panels) of cochleate samples prepared by rapid mixing immediately following preparation (A, B), 1 week later (C, D), and 1 month later (E, F). Red arrowheads point at elongated objects.*

On a time scale of a few days to a couple weeks more and more elongated object appeared in the aggregates as it was observed by phase contrast microscopy (Figure 1. C and E). High resolution topographical AFM image of these rodlike structures was consistent with the cochleate model suggested previously based on electronmicroscopy imaging (Figure 1. D and F). Besides cochleates numerous vesicles were also seen in

the sample. Few partially rolled cochleate particles were also observed (Figure 2) with an order-of-magnitude larger typical thickness of the rolling layer than that of a phospholipid bilayer. Cochleate formation was observed in aqueous medium only; when samples were dried on the AFM substrate, no further cochleates appeared in them.

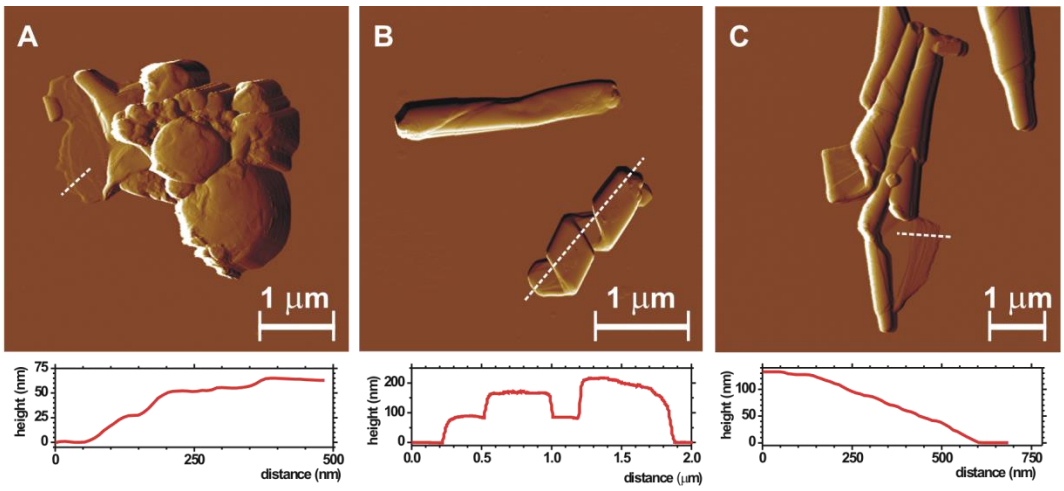

Figure 2. *AFM amplitude-contrast image of partially rolled cochleates. Height sections taken along the white dashed lines are shown below the image panels.*

4.1.2. Mechanical characterization of cochleates

AFM mechanomanipulation of individual cochleate particles revealed characteristic force spectra, which are considered to be the nanomechanical fringerprints of cochleates (Figure 3.**).**

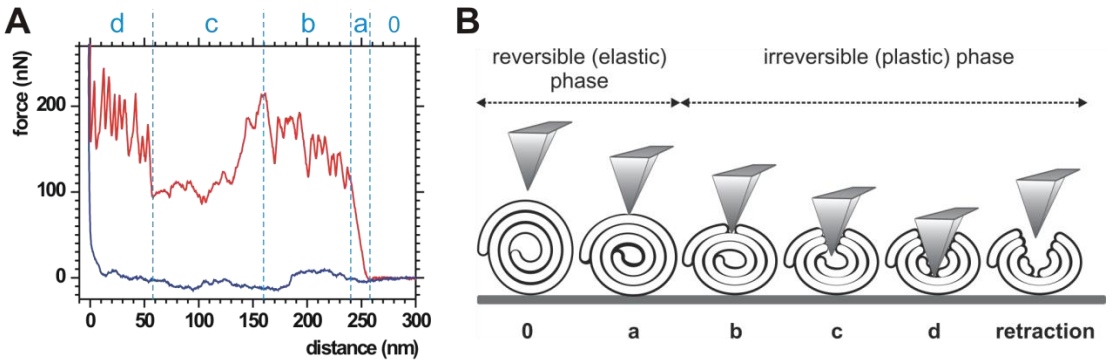

Figure 3. *(A) Representative AFM force spectrum of cochleates. Red and blue lines correspond to data collected during the cantilever approach and retraction, respectively. (B) Model of cochleate mechanomanipulation. Letters below the diagram correspond to phases shown in panel A.*

The approach curve could be divided into four distinct phases. After a featureless, constant-force region that corresponds to the unloaded movement of the cantilever towards the cochleate surface (indicated by "0"), a steep force rise emerged (phase "a") that turned into a series of sawtooth-like peaks (phase "b"). This period ended with a transient force drop and an unstructured region (phase "c") that transformed into another series of sawtooth force peaks (phase "d") before force abruptly increased. Retraction curves were featureless on this force scale, suggesting that, in this phase, there was no significant mechanical load on the cantilever. Thus, a large hysteresis appears between the approach and retraction curves. Linearity of phase „a" indicates elastic response, and the slope of this phase of the curve corresponds to the stiffness (or spring constant) of the membrane roll. Distribution of cochleate stiffness is shown in Figure 4. A. Peaks in phases „b" and „d" correspond to membrane layer breakthrough events the distribution of which is presented in Figure 4. B. When we repeated cycles of loading with excessive forces, only the first mechanical cycle displayed the characteristic mechanical fingerprint shown above. The subsequent cycles were essentially devoid of transitions and hysteresis, and the mechanomanipulation resulted in permanent depressions in the cochleate surface.

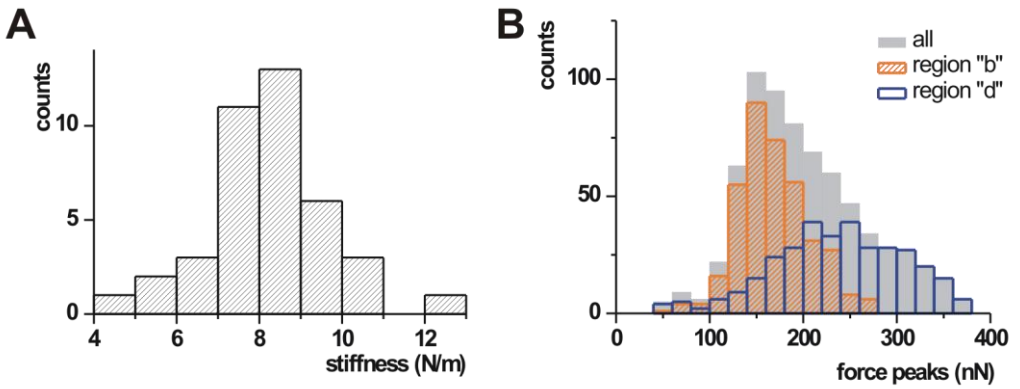

Figure 4. *(A) Histogram of cochleate stiffness (n=40). (B) Histogram of breakthrough forces of cochleate membrane layers (n_b=373 and n_d=330).*

4.1.3. Cochleate mechanics in aqueous environment

The results presented above were obtained on dried cochleate samples at ambient humidity. We also examined the morphology and mechanical properties of cochleates in aqueous environment by using AFM. We found no difference between the topography

of cochleates and their byproducts in dried and submerged samples. Likewise, their force spectra, especially the first phases of approach curves were largely similar. The main mechanical parameters of dry and fully hydrated cochleates are shown in Tabe I. It is noteworthy that signs of plastic deformation were found to be permanent and we could not observe structural restoration on a timescale of tens of minute in either of the dry ot hydrated samples.

Table I. *Mechanical properties of dry and fully hydrated cochleates (mean±SD)*

	Dry cochleates	**Fully hydrated cochleates**
Stiffness	5.08±3.69 N/m	5.17±6.61 N/m
Breakthrough forces*	81.23±18.77 nN	63.76±38.63 nN
Peak-to-peak distances	15.22±7.16 nm	17.79±10.05 nm
Line tension	approx. 1.2 nN	approx. 1.2 nN

** Mean values differ but the main peaks of their distribution coincided. Deviation is attributed to tip-adsorbed bilayer breakthrough artefact. See further details in the dissertation.*

4.1.4. Dispersion of cochleates

We hypothesized that Ca^{2+} ions in between cochleate membrane layers are less accessible to chelators than their cochlete surface-bound counterparts, which lead to cochleate aggregation. If this is true, a molecule with appropriate affinity to Ca^{2+} ions would remove ions only from the surface of cochleates leading to dispersion of aggregates without affecting the structural stability of membrane rolls. To test this hypothesis, we systematically analyzed the effect of sodium salts of acetic-, tartaric, citric- and edetic acid on aggregated cochleates. Acetate ions could not disperse aggregates up to 500 mM concentration, while tartrate ions applied in 500 mM concentration led only to partial deaggregation of the precipitates. By contrast, citrate ions led to concentration-dependent effects: in a concentration range of 0-150 mM partial deaggregation occurred, between 200 mM and 212.5 mM total dispersion was reached (Figure 5. A), and at higher concentrations more and more cochleates transformed to giant vesicles. Incubating cochleates with optimal dispersing concentration of citrate for a longer time also resulted in drastic structural changes: cochleates opened up to form giant vesicles (Figure **5**. B). However, if the citrate ions were removed from the sample immediately after dispersion, cochleates did not form

vesicles (Figure 5. C). The addition of as low as 5 mM EDTA led to the transformation of cochleates into giant vesicles.

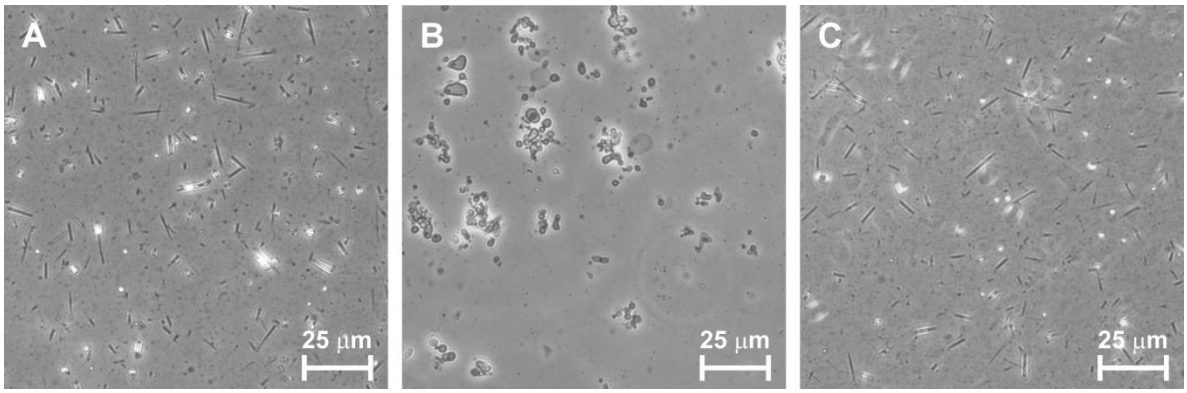

Figure 5. *Phase contrast micrographs of citrate-treated cochleate samples. (A) Cochleates dispersed in 212.5 mM sodium citrate. (B) The same sample after 24 h of incubation at room temperature. (C) Same sample as in (A) but centrifuged and resuspended in 100 mM TRIS pH=7.4 buffer immediately following citrate treatment. Nominal concentration of DOPS and* Ca^{2+} *was 3.1 mM.*

4.1.5. Effect of citrate treatment on the structure of cochleates

Structural characteristics of citrate-treated cochleates were studied by applying high-resolution AFM imaging and SAXS. Dispersed cochleates showed no considerable topographical difference compared to untreated cochleates (Figure 6.).

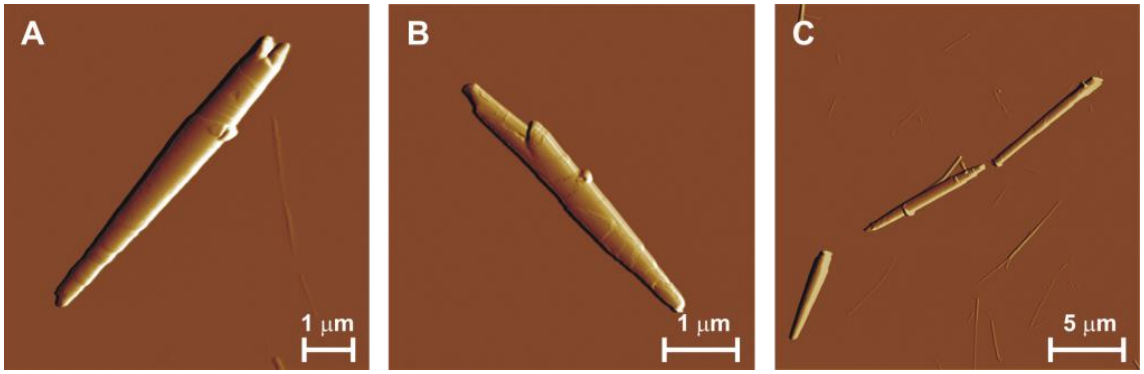

Figure 6. *AFM amplitude-contrast images of citrate-treated cochleates.*

Scattering was measured in an interval corresponding to the range of bilayer thickness and periodicity (0.3–6 nm^{-1}). The investigated samples were a DOPS multilamellar vesicle suspension, a control sample with aggregated cochleate particles, another two with 100 mM and 212.5 mM citrate, and finally one containing 50 mM EDTA instead of citrate. The hydrated DOPS system, which is expected to form

multilamellar vesicles, showed a very broad signal between 0.5 nm^{-1} < q < 3 nm^{-1} (Figure 7., spectrum „A") typical for entirely uncorrelated multilamellar systems.

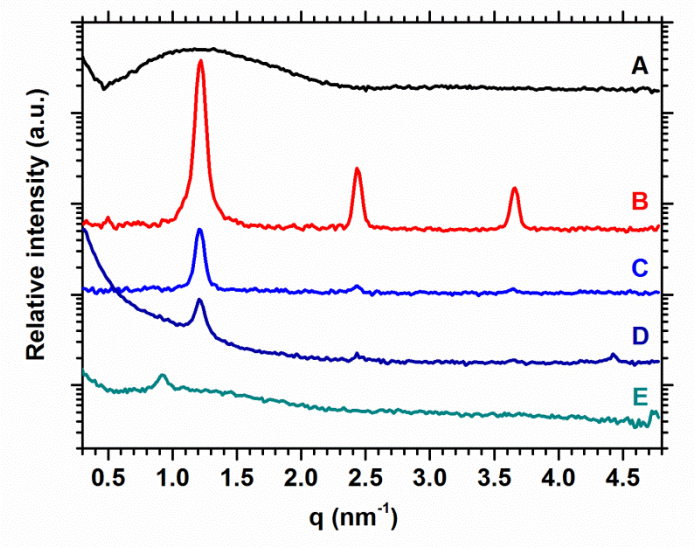

Figure 7. *SAXS spectra of (A) DOPS MLV-s, (B) control cochleates, (C) cochleates + 100 mM citrate, (D) cochleates + 212.5 mM citrate, (E) cochleates + 50 mM EDTA. Spectra are gradually shifted along the ordinate for better display.*

In the cochleate spectrum we observed a drastic change in the layer organization as seen from the sharp, equidistant Bragg-reflections at 1.2, 2.4 and 3.77 nm^{-1} (Figure 7., spectrum „B"). This reflects a highly ordered and periodic lamellar state with a repeat distance of 5.15 nm. This structure was retained even following the addition of citrate (Figure 7., spectrum „C" and „D"). The peak positions align well with those of the control cochleate sample and correspond to a 5.18 nm repeat distance. The observed loss in intensity was likely caused by the different sedimentation rate of samples which resulted in different amounts of lipid material in the lower region of the capillaries where the X-ray beam was focused. At 212.5 mM citrate concentration the SAXS signal monotonically increased towards small angle intervals, which is attributed to the diffuse scattering by the smaller particles emerging during the disaggregation process (Figure 7., spectrum „D"). This feature was absent in control cochleate (Figure **7.**, spectrum „B") and cochleate + 100 mM citrate (Figure 7., spectrum „C") samples, because the scattering by the large aggregates made little contribution in this region. The addition of EDTA induced significant changes in bilayer structure (Figure 7., spectrum „E"). The overall scattering curve resembles that of uncorrelated bilayers, and a single Bragg peak at 0.92 nm^{-1} appeared. This reflection corresponds most likely to the small amount of

regular multilamellar bilayer stacks present in the system. The periodicity (6.8 nm) is significantly greater than that in cochleates (5.15 nm) indicating that layer packing is less tight than in cochleates. In summary, applying citrate at a concentration optimal to disperse aggregated cochleates does not modify the inner structure of the membrane rolls.

4.1.6. FTIR-analysis of molecular changes of the lipid bilayer

To reveal the molecular mechanisms of the dispersing effect of citrate, we carried out infrared spectroscopy measurements with a focus on the phosphate (1250-100 cm^{-1}, Figure 8. A), methylene (3000-2800 cm^{-1}, Figure 8. B) and ester carbonyl (1760-1690 cm^{-1}, Figure 8. C) stretching vibrations which are sensitive to phosphate head group hydration, acyl-chain order and glycerol-group hydration, respectively.

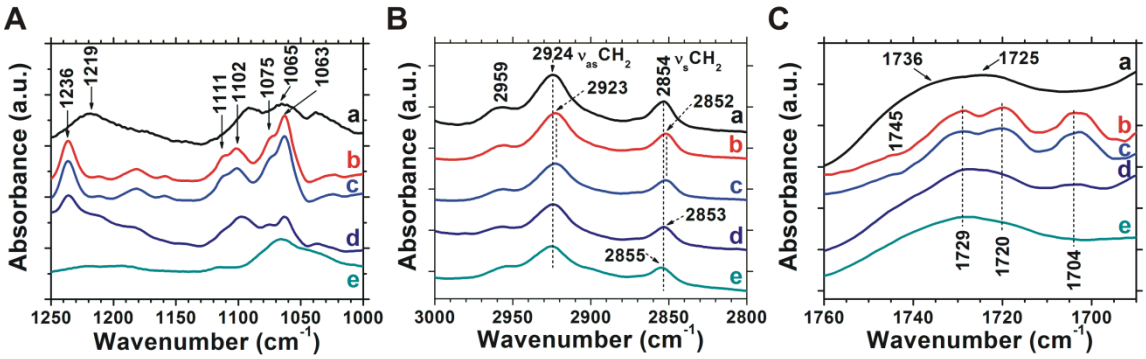

Figure 8. *The (A) phosphate, (B) C-H and (C) ester carbonyl stretching region of the infrared spectra of hydrated lipid systems (corresponding buffer spectra are subtracted). (a) DOPS SUV, (b) cochleates; (c) cochleates + 100mM citrate, (d) cochleates + 212.5 mM citrate; (e) cochleates + 50 mM EDTA.*

The asymmetric and symmetric phosphate (PO_2^-) stretching bands at 1219 and 1065 cm^{-1}, respectively, were rather featureless for the DOPS SUV system (Figure 8. A, spectrum a). In control cochleates the PO_2^- asymmetric stretching band shifted from 1219 to 1236 cm^{-1}, and the symmetric PO_2^- stretching band split into four components (1111, 1102, 1075 and 1063 cm^{-1}, Figure 8. A, spectrum b). These changes point at the dehydration of the phosphate group and the formation of a bidentate complex between the Ca^{2+} ion and the phosphate ester. Addition of 100 mM citrate did not cause any spectral changes in the phosphate head group region (Figure 8. A, spectrum c). At 212.5 mM citrate concentration the relative intensities of phosphate stretching bands, characteristic to Ca^{2+}–DOPS interaction, decreased (Figure 8. A, spectrum d), implying

that a fraction of Ca^{2+}–phosphate complexes dissociated. Addition of 50 mM EDTA led to the disappearance of the characteristic phosphate bands of Ca^{2+}-phosphate interaction. Note that both citrate and EDTA have absorption bands in this region, the subtractions of which decreased the quality of the spectra.

In DOPS liposomes antisymmetric ($\nu_{as}CH_2$) and symmetric (ν_sCH_2) methylene stretching vibrations dominated at 2924 and 2854 cm^{-1}, respectively (Figure 8. B, spectrum a). In control cochleates the methylene stretching band positions shifted towards lower wavenumbers (Figure 8. B, spectrum b) indicating a tighter lipid packing, which may be attributed to the strong interaction of Ca^{2+} with lipid head groups. Addition of 100 mM citrate had no observable effect in this spectral region (Figure 8. B, spectrum c). However, at a dispersing citrate concentration (212.5 mM) the position of both the asymmetric and symmetric stretching bands shifted to higher wavenumbers approaching those of the Ca^{2+}-free liposomes (Figure 8. B, spectrum d). Thus, a fraction of lipids became less tightly packed. Upon adding 50 mM EDTA, a further increase of ν_sCH_2 could be observed as a result of acyl-chain perturbation leading to a lipid bilayer structure, the packing of which is similar to that of liposomes (Figure 8. B, spectrum e). In the spectral region sensitive to ester carbonyl vibrations, DOPS liposomes (Figure 5. C, spectrum a) displayed a broad band that could be deconvoluted into two components (at ~1736 cm^{-1}, and at ~1725 cm^{-1}) assigned to differently hydrated subpopulations of the two carbonyl groups. Upon Ca^{2+} addition, four νC=O stretching bands became distinct at 1745, 1729, 1720 and 1704 cm^{-1} (Figure 8. C, spectrum b). The lower wavenumbers point at the formation of new hydrogen bonds, while band narrowing is due to a significant reduction in motional freedom caused most likely by the immobilization of polar headgroups due to Ca^{2+} complexation. Addition of 100 mM citrate did not alter the IR spectrum (Figure 8. B, spectrum c). At the dispersing citrate concentration (212.5 mM), however, the intensities of the narrow νC=O stretching bands, specific to the Ca^{2+}–DOPS complexes, decreased, and a broad band centered at 1728 cm^{-1}, characteristic to hydrated DOPS lipids. Upon the addition of 50 mM EDTA the carbonyl stretching region of the IR spectrum reverted back to that of DOPS liposomes, and the spectral features characteristic to cochleates disappeared.

5. Conclusion

5.1. Formation of cochleates

Models describing the formation of cochleates need to be revised. Ca^{2+}-mediated fusion and aggregation of unilamellar liposomes lead to multilamellar vesicle aggregates and not to planar phospholipid bilayers or multilamellar stacks of them as suggested earlier. Since practically there are no cochleates in the fresh aggregates, but in a few days they appear and their number increases, we hypothesize that these are the multilamellar vesicles which transform to cochleates with an unknown mechanism. Because the number of cochleates increases relatively slowly in the sample but no intermediate phase of cochleate formation could be unequivocally identified, MLV→cochleate transition is postulated to be a quick, unidirectional, stochastic process. Analysis of partially rolled structures revealed that in most cases not a single but multiple parallel phospholipid membrane bilayers roll up to cochleates. Blocking of MLV→cochleate transition by drying of the sample indicates that aqueous medium has important role in cochleate formation. To understand the exact mechanism of the transition further studies are needed.

5.2. Structural and mechanical properties of cochleates

Atomic force microscopy proved to be valuable to examine the topography and characteristics of the inner structure of cochleates at high resolution. AFM images underpinned the structural modell of cochleates proposed earlier, and showed that membrane rolls may contain a hollow core. A nanomechanical fringerprint of cochleates revealing their internal structure and mechanical properties can be identified by single-particle force spectroscopy. Membrane rolls display extraordinary stiffness values (approx. 1-15 N/m) compared to other ordered biomolecular systems. Exceedingly large forces (from tens to few hundreds of nN) are needed to break through them, leading to – in the time sclale of the experiments – plastic deformation. Because the mechanical parameters of dry and fully hydrated cochleates are essentially identical, the aqueous medium does not play role in the stabilization of the already formed membrane rolls. Line tension of individual bilayers (approx. 1.2 nN) exceeds that of liquid-crystalline phospholipid bilayers by orders of magnitude. This and the lack of reordering of

membranes after breakthrough proves that bilayers are in a quasicrystalline phase in cochleates.

Individual membrane bilayers behave independently from each other during breakthrough, pointing at the lack of mechanical coupling between them. This may have two reasons: *(1)* It is possible that the headgroups of phospholipids in adjacent layers do not bind to each other via Ca^{2+} bridges as it was suggested earlier. Large number of parallel Ca^{2+} crossbridges should provide very strong coupling between neighboring layers, a scenario which could not lead to independent, equal-force transitions, unless if we postulate that Ca^{2+} crossbridges are able to reorganize dynamically. In the latter case, however, we would expect for the reorganization of the layers that were broken through by the AFM tip – something we did not observe. It seems plausible that Ca^{2+} interconnect neighboring phospholipid headgroups only within a membrane layer. The resultant, largely dehydrated, charge-screened headgroup layers may associate to adjacent layers via *van der Waals* or hydrophobic interactions. *(2)* It is possible that the sliding of the layers on each other during mechanomanipulation takes place within the plane of the fatty acid tails of phospholipids.

5.3. Dispersion of cochleates

Citrate has a concentration-dependent effect on cochleate aggregates: at low concentrations it loosens their structure, at optimal concentration it disperses them, while at higher concentrations membrane rolls open up. This effect is attributed to the ability of citrate ions to bind a fraction of freely-dissolved Ca^{2+} ions, lowering their concentration, which shifts the PS–Ca^{2+} binding equlibrium towards dissociation. From this aspect the PS–Ca^{2+} complexes of cochleates can be categorized into two groups: *(1)* a superficial, easily accessible, and *(2)* an inner, sterically hidden fraction.

Dissociation of Ca^{2+} from PS headgroups and its diffusion to the solution is determined by the potential gradient between the solution and the cochleate. Association constant of citrate ions (pK_a=3.17) is smaller but comparable to that of the PS molecule (pK_a=3.9). Citrate ions and PS headgroups compete for free Ca^{2+} ions. Citrate ions have to be applied in a concentration higher than the PS concentration in order to complex enough free Ca^{2+} ions to shift the dissociation equilibrium and thus the potential gradient in an extent appropriate to lead to the dissociation of superficial PS–Ca^{2+}

complexes during the relatively short incubation time. Moderate chemical potential gradient does not allow inner Ca^{2+}–PS complexes to dissociate before the removal of the dispersing agent by buffer exchange. Without buffer exchange even the optimal concentration of citrate extracts Ca^{2+} ions from the interior of the membrane rolls over longer time. EDTA, which has much larger Ca^{2+}-association constant (pK_a=10.75), binds Ca^{2+} with orders of magnitude higher affinity, resulting in a sudden, enormous increase of Ca^{2+} chemical potential gradient. This shifts the binding equilibrium of PS–Ca^{2+} complexes in such a large extent, and accelerates the withdrawal of Ca^{2+} ions from inside the cochleates, that their characteristic roll structure opens up almost instantenously. Tartaric and acetic acid having much lower pK_a (1.8 and 0.53, respectively) cannot extract enough Ca^{2+} ions from the particles to disperse them, even if applied at relatively high concentration.

5.4. Novel scientific results

(1) I observed that cochleate formation from unilamellar liposomes first results in aggregates of multilamellar vesicles. Later these vesicles transform to membrane rolls in a unidirectional, quick, stochastic process. For the multitude of particles transformation follows relatively slow kinetics, it takes a few weeks for cochleates to prevail over vesicles. Vesicle→cochleate transition takes place in aqueous medium only.

(2) I identified, by AFM force spectroscopy, the nanomechanical fringerprint of cochleates, which reflects the structural and mechanical properties of membrane rolls. Cochleates exhibit extreme stiffness and mechanical resilience compared to other ordered biomolecular nanostructures. Line tension of cochleate lipid bilayers was found to be approximately 1.2 nN, a value large enough to provide indirect proof of phospholipid membrane crystallization. This is also supported by plastic deformation of cochleates. Cochleate membrane layers are not coupled to each other mechanically, which makes probable that i.) Ca^{2+} ions form crossbridges between phospholipid headgroups within the same layer, and ii.) adjacent layers are coupled to each other by *van der Waals* and hydrophobic interactions.

(3) I developed a method to disperse cochleate aggregates, based on applying of citrate ions in appropriate concentration followed by buffer exchange. This way citrate ions do not damage the characteristic structure of cochleates. Molecular background of structure-preserving dispersion method is that citrate removes Ca^{2+} ions solely from cochleate surface, without extracting the Ca^{2+} ions stabilizing the inner layers of cochleates.

6. Publications

6.1. Publications related to the present thesis

Bozó, T, Wacha, A, Mihály, J, Bóta, A, Kellermayer, MSZ (2017) *Dispersion and stabilization of cochleate nanoparticles*. Eur J Pharm Biopharm, 117:270-275. IF: 4.159

Bozó, T, Brecska, R, Gróf, P, Kellermayer, MSZ. (2015) *Extreme resilience in cochleate nanoparticles*. Langmuir 31:839-845. IF: 3.993

6.2. Publications not related to the present thesis

Batta, Gy, Soltész L, Kovács, T, **Bozó, T**, Mészár, Z, Kellermayer, MSZ, Szöllősi J, Nagy, P. (2018) *Alterations in the properties of the cell membrane due to glycosphingolipid accumulation in a model of Gaucher disease.* Sci Rep 8:157. IF: 4,259

Tóth, EA, Oszvald, Á, Péter, M, Balogh, G, Osteikoetxea-Molnár, A, **Bozó, T**, Szabó-Meleg, E, Nyitrai, M, Derényi, I, Kellermayer, M, Yamaji, T, Hanada, K, Vígh, L, Matkó, J. (2017) *Nanotubes connecting B lymphocytes: High impact of differentiation-dependent lipid composition on their growth and mechanics*. BBA- Mol Cell Biol L 1862: 991-1000. IF: 5,547

Bozó, T, Meszáros, T, Mihály, J, Bóta, A, Kellermayer, MSZ, Szebeni, J, Kálmán, B. (2016) *Aggregation of PEGylated liposomes driven by hydrophobic forces*. Colloids Surf B Biointerfaces 147:467-474. IF: 3.887

Osteikoetxea-Molnar, A, Szabó-Meleg, E, Tóth, EA, Oszvald, Á, Izsépi, E, Kremlitzka, M, Biri, B, Nyitray, L, **Bozó, T**, Németh, P, Kellermayer, MSZ, Nyitrai, M, Matkó, J. (2016) *The growth determinants and transport properties of tunneling nanotube networks between B lymphocytes*. Cell Mol Life Sci 73:4531-4545. IF: 5.788

Horváth, Gy, Kemény, A, Barthó, L, Molnár, P, Deli, J, Szente, L, **Bozó, T**, Pál, Sz, Sándor, K, Szőke, É, Szolcsányi, J, Helyes, Zs. (2015) *Effects of some natural carotenoids on TRPA1- and TRPV1-induced neurogenic inflammatory processes in vivo in the mouse skin*. J Mol Neurosci 56:113-121. IF: 2.352

Pál, Sz, Nagy, S, **Bozó, T**, Kocsis, B, Dévay, A. (2013) *Technological and biopharmaceutical optimization of nystatin release from a multiparticulate based bioadhesive drug delivery system*. Eur J Pharm Sci 49:258-264. IF: 3.005

Kaszás, N, **Bozó, T,** Budai, M, Gróf, P. (2013) *Ciprofloxacin encapsulation into giant unilamellar vesicles: Membrane binding and release*. J Pharm Sci 102:694-705. IF: 3.007

Bozó, T, Mayer, K, Pál, S, Dévay, A. (2009) *A szem korszerű gyógyszeres terápiájának lehetőségei*. Gyógyszerészet 53:5-12. (In Hungarian)

Bozó, T, Pál, S, Dévay, A. (2008) *Liposzómák fejlesztésének és gyógyszerterápiás alkalmazásának újabb lehetőségei*. Acta Pharm Hung 78:103-109. (In Hungarian)